THE SEA: THE CURRENT AND FUTURE OCEAN
Journal of Marine Research, 77, Supplement, 191–213, 2019

Amazon River influence on nitrogen fixation in the western tropical North Atlantic

by Joseph P. Montoya,[1,2] Jason P. Landrum,[1,3] and Sarah C. Weber[1,4]

ABSTRACT

We measured rates of N- and C-fixation with a direct tracer method in regions of the western tropical North Atlantic influenced by the Amazon River plume during the high flow period of 2010 (May–June 2010). We found distinct regional variations in N-fixation activity, with the lowest rates in the plume proper and the highest rates in the plume margins and in offshore waters. A comparison of our N- and C-fixation measurements showed that the relative contribution of N-fixation to total primary production increased from the plume core toward oceanic waters, and that most of the C-fixation in this system was supported by sources of nitrogen other than those derived from biological N-fixation, or diazotrophy. We complemented these rate experiments with measurements of the $\delta^{15}N$ of suspended particles ($\delta^{15}PN$), which documented the important and often dominant role of diazotrophs in supplying nitrogen to particulate organic matter in the water column. These coupled measurements revealed that small phytoplankton contributed more new nitrogen to the particulate nitrogen pool than larger phytoplankton. We used a habitat classification method to assess the factors that control diazotrophic activity and contribution to the suspended particle pool, both of which increased from the plume toward oceanic waters. Our findings provide an important constraint on the role of the Amazon plume in creating distinct niches and roles for diazotrophs in the nutrient and carbon budgets of the western tropical North Atlantic.

Keywords: Nitrogen fixation, tropical North Atlantic, Diazotrophy, Nitrogen stable isotopes

1. Introduction

The Amazon River is the largest single source of fresh water entering the ocean, amounting to almost 20% of the global riverine input to the ocean (Vorosmarty et al. 2000). This freshwater flow generates a surface plume that extends well offshore into the western tropical North Atlantic, or WTNA (Del Vecchio and Subramaniam 2004; Hu et al. 2004; Molleri, Novo, and Kampel 2010). The path of the Amazon plume varies seasonally, trending to the

1. School of Biological Sciences, Georgia Institute of Technology, Atlanta, GA 30332 USA; orcid: 0000-0001-7197-4660
2. Corresponding author: ***e-mail: montoya@gatech.edu***
3. Lenfest Ocean Program, The Pew Charitable Trusts, 901 E Street NW, 10th Floor, Washington, DC 20004 USA; orcid: 0000-0003-1614-7261
4. Department of Marine Biology, Leibniz-Institute for Baltic Sea Research Warnemünde, D-18119 Rostock, Germany; orcid: 0000-0002-0612-5598

northwest in the winter and spring and retroflecting eastward into the central equatorial Atlantic during the summer and fall (Muller-Karger, McClain, and Richardson 1988; Johns et al. 1990; Coles et al. 2013). The impact of the Amazon plume on planktonic productivity has been debated, with some early observations suggesting that the plume might have a negative impact on productivity (e.g., Ryther, Menzel, and Corwin 1967). Other researchers have suggested that the plume might promote blooms of both phytoplankton (e.g., Longhurst 1993) and zooplankton (e.g., Calef and Grice 1967), and more recent expeditions have clearly documented the profound impact of the river outflow on phytoplankton communities (Goes et al. 2014) and biogeochemical processes (Yeung et al. 2012; Stukel et al. 2014; Weber et al. 2017) of the WTNA. Specifically, the Amazon plume stimulates primary production and biological N-fixation (diazotrophy) in a region extending hundreds of kilometers from the coast (Muller-Karger, Richardson, and McGillicuddy 1995; Subramaniam et al. 2008; Weber et al. 2017).

A variety of diazotrophs (N-fixing organisms) are active in the waters affected by the Amazon plume, supplying new nitrogen that supports high rates of primary production in the region (Carpenter et al. 1999; Carpenter, Subramaniam, and Capone 2004; Foster et al. 2007; Subramaniam et al. 2008). The interactions between the Amazon plume and the surrounding oceanic waters generate a dynamic patchwork of physical and chemical conditions that in turn are associated with distinct phytoplankton assemblages, including large populations of diatom-diazotroph associations (DDAs) in and around the plume, and colonial filamentous cyanobacteria of the genus *Trichodesmium* in oceanic waters (Carpenter et al. 1999; Carpenter, Subramaniam, and Capone 2004; Foster et al. 2007; Subramaniam et al. 2008). These phytoplankton assemblages tend to occur in different portions of the salinity gradient generated by the flow and mixing of the plume and surrounding waters (Goes et al. 2014; Weber et al. 2017), but other factors including the broader physical and chemical environment (Weber et al. 2019), zooplankton grazing (Conroy et al. 2016; Loick-Wilde et al. 2016), and the persistence of appropriate habitats (Stukel et al. 2014) all appear to be important in structuring the phytoplankton community and distribution of diazotrophic activity of this region.

N-fixation adds to the local pool of biologically available nitrogen, but the fate of that nitrogen and the new production it supports are strongly dependent on the identity of the diazotrophs involved. For example, zooplankton grazing is an important pathway for moving DDA nitrogen into the food web (Conroy et al. 2016; Loick-Wilde et al. 2016). The dense silica frustules of the diatom partner in DDAs promote vertical export of new production in fecal pellets and through sinking of senescent DDA blooms (Subramaniam et al. 2008; Yeung et al. 2012). *Trichodesmium*, in contrast, is not widely grazed (Capone et al. 2005) and appears to be much less effective in promoting vertical export than DDAs (Weber et al. 2017) or small diazotrophs (Berthelot et al. 2015). Resolving the distribution and activity of different diazotroph assemblages is a critical prerequisite to any quantitative understanding of the nitrogen budget of the Amazon plume region and likely other tropical river plume systems.

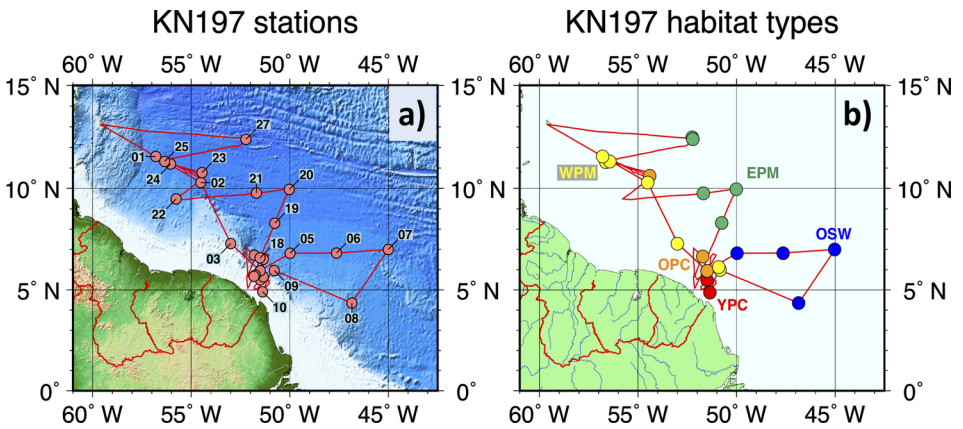

Figure 1. Cruise track of R/V *Knorr* cruise KN197-8 in spring 2010 in the western tropical North Atlantic (a) and habitat types for major stations as defined by Weber et al. (2019). Major stations are marked with red circles in panel (a). Habitat types are color coded in panel (b) as in Weber et al. (2019): red = Young Plume Core (YPC), orange = Old Plume Core (OPC), yellow = Western Plume Margin (WPM), green = Eastern Plume Margin (EPM), and blue = Offshore Waters (OSW).

We used a combination of instantaneous rate and integrative stable isotope measurements to assess the contribution of diazotrophy to the nitrogen budget of the WTNA. In doing so, we build on the multiscale approach to studying the nitrogen cycle developed by James McCarthy and his group in the 1980s and 1990s. Our field sampling and experiments were part of the multidisciplinary ANACONDAS program (Amazon influence on the Atlantic: Carbon export from nitrogen fixed by diatom symbioses), during which we sampled a broad range of conditions, from waters associated with the core of the Amazon plume to offshore waters representative of the tropical Atlantic. We carried out rate measurements and collected samples for stable isotope analysis at all of our major stations, providing complementary instantaneous and integrative measures of the nitrogen cycle. Here we discuss our rate and isotopic measurements in the context of environmental variability in the Amazon plume region to explore the factors that promote diazotrophy in these and other tropical waters.

2. Materials and methods

a. Hydrographic properties and habitat types

We collected seawater and suspended particle samples in the Amazon plume region during cruise KN197-8 (R/V *Knorr*, 22 May 2010–24 June 2010; Fig. 1a). Our 25 stations sampled a range of habitats, including waters in the core of the plume and offshore waters typical of the tropical Atlantic, and our cruise track crossed the plume core four times at different latitudes.

We obtained hydrographic data and seawater samples using a conductivity-temperature-depth rosette system equipped with a fluorometer and PAR (photosynthetically active radiation) sensor. We measured nutrient concentrations ($NO_3^- + NO_2^-$, PO_4^{3-}, and SiO_2) at sea using a Lachat QuickChem 8000 FIA system and assessed mixing of plume and offshore waters as described by Weber et al. (2017). We collected suspended particles for elemental and isotopic analysis by filtering 2–18 L of seawater through precombusted (450°C for 2 h) 47 mm GF/F filters under gentle pressure (5–10 psi). Sample filters were dried at sea (60°C) and stored over desiccant for analysis ashore.

We classified our stations using the habitat types defined by Weber et al. (2019). In brief, these habitats are defined using a principal components analysis of simple physical and chemical properties (surface salinity, surface temperature, mixed layer depth, depth of the chlorophyll maximum, and an index to nitrate availability at the surface). This analysis generated five distinct habitats in our system (Fig. 1b), which provided a robust framework for describing the distribution of phytoplankton communities: Young Plume Core (YPC), Old Plume Core (OPC), Western Plume Margin (WPM), Eastern Plume Margin (EPM), and Offshore Waters (OSW).

b. N-fixation rate measurements

We collected water for our rate measurements from four to six depths spanning the upper water column and typically extending to below the subsurface chlorophyll maximum. All of our experiments were started in the morning, typically between 07:00 and 10:00 local time (15 experiments). Four experiments were started earlier in the day (05:30–07:00 local time), and four experiments were started between 10:00 and 11:15 local time. We used the protocol of Montoya et al. (1996) to measure the rate of N-fixation using trace additions of $^{15}N_2$ gas. In brief, we carried out triplicate incubations at four to six depths extending from the surface to below the subsurface chlorophyll maximum if present. In deeper water columns, our incubations generally included the surface, the base of the mixed layer, the chlorophyll maximum, and the lower base of the pigment maximum. We used gas tight syringes to add $^{15}N_2$ (99 atom%, Cambridge Isotope) and ^{13}C-bicarbonate (99 atom%, Cambridge Isotope) to produce equilibrium enrichments of ~7 at-% $^{15}N_2$ and 2 at-% ^{13}C-DIC (dissolved inorganic carbon). Bottles were incubated under simulated in situ light conditions in flowing seawater deck incubators for 24 h and then terminated by gentle pressure filtration through a 10 μm Nitex prefilter and a precombusted (450°C for 2 h) 25 mm GF/F filter. Material captured on the prefilter was rinsed off and transferred to a precombusted (450°C for 2 h) GF/C or GF/A filter. All sample filters were transferred to small centrifuge tubes, dried at 60°C at sea, and then capped and stored over desiccant for analysis ashore.

We calculated N-fixation rates by isotope mass balance as described in Montoya et al. (1996). We used the same isotope mass balance approach to calculate C-fixation rates from ^{13}C incorporation into organic matter, estimating the ambient concentration of DIC based

on salinity (Parsons Maita, and Lalli 1984). Our experiments provide specific rates (h^{-1}) of activity normalized to the standing stock of the target pool of either N or C over the entire incubation period (~ 24 h). These daily rates integrate through a complete diel cycle and allow direct comparison of measured N- and C-fixation rates. We calculated volumetric rates of activity (nmol L^{-1} h^{-1}) by multiplying our biomass specific rates by the concentration of particulate nitrogen (PN) or carbon.

We are mindful of concerns that our experimental approach may lead to bias in our rate estimates (e.g., Mohr et al. 2010; Grosskopf et al. 2012) because of incomplete equilibration of the injected bubble of $^{15}N_2$. Our own comparisons at sea suggest that any potential underestimate is negligible for 24 h incubations, and a formal meta-analysis of available data coupled with experimental measurements and calculations of equilibration time show no significant differences between the bubble and enriched water methods for incubations of this length (Wannicke et al. 2018). In practical terms, the physical and temporal heterogeneity of the Amazon plume region makes it very challenging to efficiently use the equilibrated water approach of Glibert and Bronk (1994) or Mohr et al. (2010) in place of the much simpler bubble method, which requires very little handling and minimizes the potential for altering the chemical environment within the incubation bottle through addition of exogenous nutrients or other compounds.

c. Elemental and isotopic analyses

We carried out our stable isotope abundance measurements by continuous-flow isotope-ratio mass spectrometry using a Micromass Optima interfaced to a Carlo Erba NA2500 elemental analyzer for online combustion and purification of sample nitrogen and carbon. We report stable isotope abundances as $\delta^{15}N$ values relative to atmospheric N_2. We used both elemental (acetanilide and methionine) and isotopic (peptone) standards to check instrument stability and to correct for analytical blanks as described by Montoya (2008). We conservatively estimate that the overall analytical precision of our isotopic measurements is better than ± 0.1‰.

d. Water column rates and means

We used trapezoidal integration to calculate water column (areal) rates of N- and C-fixation. For each station, we also used Redfield stoichiometry (C:N = 6.7) to estimate the percentage of the measured areal C-fixation rate that could be supported by the areal rate of N-fixation. Finally, we calculated a mass- and depth-weighted mean $\delta^{15}N$ for particles in the upper water column as described by Landrum, Altabet, and Montoya (2011).

e. Isotope mixing model

We used a nitrogen isotope mass balance approach (Montoya, Carpenter, and Capone 2002) and the end members used by Weber et al. (2017) to calculate the contribution of diazotroph nitrogen to suspended particles (N_{diazo}) in the upper water column. As noted

by Weber et al. (2017), the isotopic systematics are simplified by the similar $\delta^{15}N$ (4.5‰–5.0‰) of particles at the southern end of our survey area and subsurface NO_3^- in the Atlantic (Sigman et al. 2000; Loick-Wilde et al. 2016). The other major nitrogen source for the surface waters of the plume is N-fixation, which contributes N with a $\delta^{15}N$ of –2‰ (Montoya et al. 2002). This produced a simple linear mixing model to estimate % N_{diazo} from $\delta^{15}N$:

$$\%\ N_{diazo} = 100 \cdot \frac{\delta^{15}N_{particles} - \delta^{15}N_{(nitrate\ +\ organic\ N)}}{\delta^{15}N_{diazo} - \delta^{15}N_{(nitrate\ +\ organic\ N)}} \quad (1)$$

where $\delta^{15}N_{(nitrate + organicN)} = 5‰$ and $\delta^{15}N_{diazo} = -2‰$.

3. Results

a. Hydrographic properties and habitat types

As described by Weber et al. (2017), plume thickness and width varied along our cruise track, with the greatest extent toward the northern portion of our study area. We found substantial variation in the distribution of hydrographic properties on timescales of hours to days, reflecting the highly dynamic interactions between the plume and its surrounding waters. Of the major nutrients, only silicate showed a classic pattern of variation with salinity, while nitrate concentrations were low or below the limit of detection throughout our study region and phosphate concentrations varied widely, with many positive deviations from conservative mixing (Weber et al. 2017). Interestingly, the positive phosphate anomalies tended to increase with distance down the plume axis (fig. 2 of Weber et al. 2017), consistent with release of phosphate into the water column as the plume waters aged and interacted with the surrounding oceanic waters.

We categorized our stations using the five habitat types defined by Weber et al. (2019), which have already proved useful in delineating phytoplankton assemblages in this system. The five habitat types for this system form a sequence extending from the plume proper (YPC and OPC) to regions where the plume interacts with surrounding oceanic waters (OSW) at the western (WPM) and eastern (EPM) sides of the plume axis. The five habitat types are spatially intermingled to some extent (Fig. 1b), reflecting the dynamic nature of the plume and its surroundings.

b. Rates of N- and C-fixation

We found measurable rates of N- and C-fixation throughout our study region with clear vertical structure and marked variation among stations (Fig. 2, Table 1). In general, volumetric N-fixation rates (range: 0–0.55 nmol L^{-1} h^{-1}, N = 123) were highest near the surface and decreased with depth, though the depth interval with elevated N-fixation rates differed among habitat types. The strongest depth stratification was associated with the WPM stations, while the EPM and OSW stations tended to show elevated rates over a greater depth range. In most habitat types, the highest volumetric rates of N-fixation were associated with

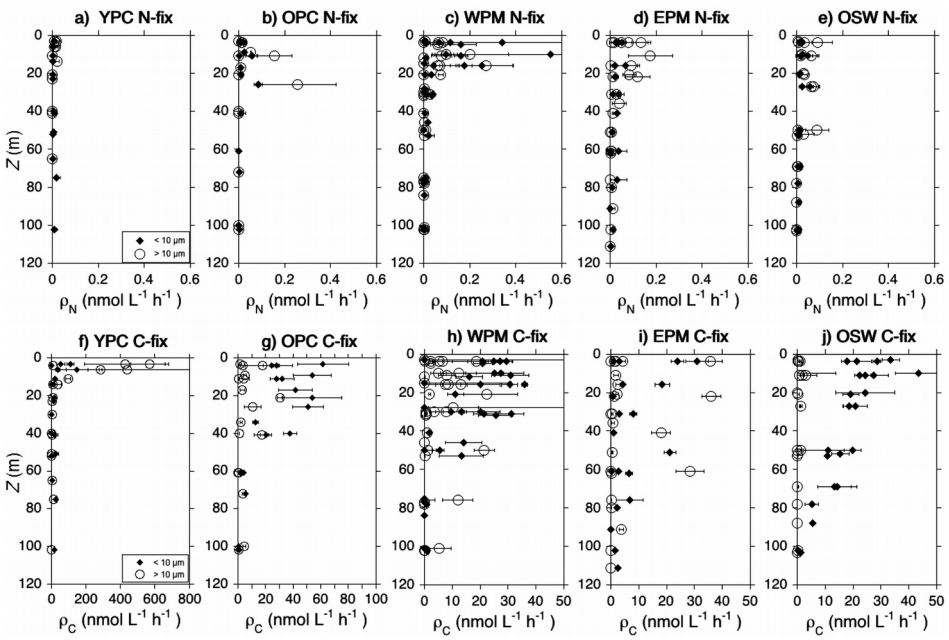

Figure 2. Vertical distribution of volumetric N-fixation rates (panels a–e, mean ± standard deviation [SD]) and C-fixation rates (panels f–j, mean ± SD) separated by habitat type. In each panel, the activity of the small size fraction of plankton is shown with a solid diamond and the activity of the large size fraction of plankton (> 10 µm) is shown by a large open circle. Note that the horizontal scale for C-fixation rate varies among habitat types.

the large size fraction (Fig. 2a, b, d, and e), though the WPM stations differed in this respect as well, with elevated rates in the small size fraction of particles (Fig. 2c).

The areal rates of N-fixation by both size fractions of plankton were low in the freshest waters sampled, with both the mean rate and the variance among stations increasing with increasing salinity (Fig. 3a). When separated by habitat type, areal N-fixation rates were generally lowest in the plume core (YPC and OPC) and elevated in the plume margins and offshore waters (Figs. 4a–c and 5). The WPM samples showed the greatest variation in areal N-fixation by the small size fraction and in total community N-fixation rate (Figs. 4 and 5).

Volumetric C-fixation rates ranged from undetectable to more than 700 nmol L^{-1} h^{-1} ($N = 123$) and were highest in the plume proper (YPC surface waters), where we found very high activity by large plankton in the upper 10 m of the water column (Fig. 2f). C-fixation rates decreased with depth at most stations, though the rate of decrease with depth varied among habitat types (Fig. 2).

Areal rates of C-fixation by small particles showed little change with salinity (Fig. 3b), whereas large particles showed very high rates of C-fixation at the lowest salinities. As a result, the total areal rate of C-fixation decreased markedly as salinity increased in our

Table 1. Summary of integration depths used in calculating areal rates and water column mean $\delta^{15}N$, total areal rates of N- and C-fixation, relative contribution of diazotrophy to C-fixation, and diazotroph contribution to suspended particulate nitrogen (PN). For each parameter, the mean ± standard error is shown in the first line, and the range of values observed is shown in parentheses on the second line. EPM, Eastern Plume Margin; OPC, Old Plume Core; OSW, Offshore Waters; WPM, Western Plume Margin; YPC, Young Plume Core.

Habitat type (N)	Integration depth (m)	N-fixation rate (μmol m^{-2} d^{-1})	C-fixation rate (mmol m^{-2} d^{-1})	Diazotrophy, C-fixation contribution (%)	Diazotrophy, PN contribution (%)
YPC	73.1 ± 18.2	17.2 ± 7.1	106.7 ± 35.5	0.16 ± 0.12	4.7 ± 3.3
(N = 3)	(52–102)	(8.6–28.3)	(53.8–153.5)	(0.04–0.35)	(0.0–9.6)
OPC	101.3 ± 0.8	75.9 ± 67.0	57.5 ± 13.6	0.9 ± 0.9	32.9 ± 8.5
(N = 3)	(100–102)	(20.9–185.3)	(41.1–78.6)	(0.2–2.4)	(23.8–46.6)
WPM	95.9 ± 4.2	118.3 ± 41.6	43.7 ± 8.9	2.7 ± 1.3	46.5 ± 13.2
(N = 7)	(78–102)	(12.0–320.5)	(22.7–81.4)	(0.1–9.5)	(15.1–100.0)
EPM	133.4 ± 8.3	97.3 ± 13.9	19.5 ± 11.7	14.1 ± 8.0	69.4 ± 7.6
(N = 5)	(121–152)	(66.9–130.2)	(2.0–56.6)	(0.8–39.7)	(52.8–89.9)
OSW	101.7 ± 0.7	104.7 ± 30.3	37.4 ± 2.7	1.9 ± 0.5	95.7 ± 3.6
(N = 4)	(100–103)	(58.4–166.6)	(31.6–41.8)	(0.9–2.8)	(86.7–100.0)

work area (Fig. 3b). When we partitioned our samples by habitat type, we found a general decrease in total C-fixation rates from the plume core to the plume margins and offshore waters (Figs. 3 and 4).

c. Diazotroph impacts

The weighted mean $\delta^{15}N$ of suspended particles ($\delta^{15}PN$) ranged from −2.9‰ to 5.0‰ and decreased strongly with increasing rates of N-fixation (Fig. 6). The water column mean $\delta^{15}PN$ showed a stronger dependence on the areal rate of N-fixation by small particles than on the areal rate of N-fixation by large particles. As expected, the relationship between mean $\delta^{15}PN$ and total areal N-fixation rate was intermediate between the small and large size fraction cases.

We quantified the role of diazotrophy in supporting the production of biomass in the Amazon plume region by applying a linear mixing model (equation 1) to the mean water column $\delta^{15}N$ of suspended particles, following the work of Landrum, Altabet, and Montoya (2011) in the Sargasso Sea. The diazotrophic contribution to water-column-suspended particles ($\%N_{diazo}$) ranged from 0 to 100% with marked differences among habitat types (Fig. 7a). The YPC waters showed the lowest diazotroph contribution. The diazotroph contribution to suspended particles increased from YPC to OPC and plume margin waters, with the very highest diazotroph contributions in our OSW stations (Fig. 7a). The WPM stations showed the greatest variability among stations, whereas the other

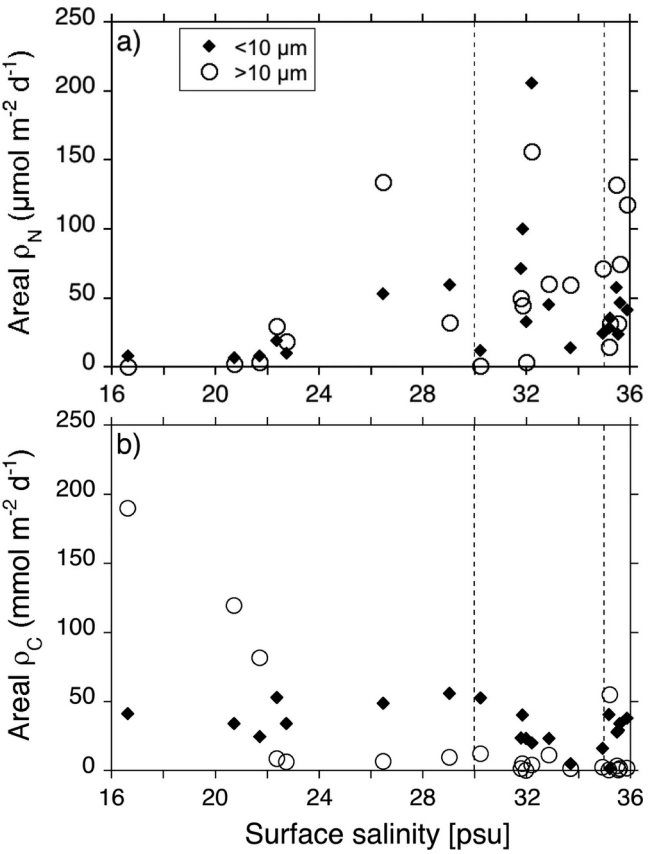

Figure 3. Areal rates of N-fixation (a) and C-fixation (b) as a function of salinity. In each panel, rates associated with the small size fraction of particles are shown with a solid diamond, and rates associated with the large size fraction are shown with a large open circle.

four habitat types showed relatively little variation in diazotroph contribution among stations.

We assessed the contribution of diazotrophs to primary production by comparing areal rates of N- and C-fixation based on Redfield stoichiometry. At most stations, diazotroph C-fixation was a small fraction ($< 5\%$) of primary production by small phytoplankton, and diazotrophs made larger contributions to primary production by small cells at only one WPM and two EPM stations (Fig. 7b). In contrast, diazotrophs accounted for more than 10% and up to 47% of the C-fixation by large phytoplankton at 10 stations distributed among all but the YPC habitat type (Fig. 7b). We found the greatest range of N-fixation contributions to primary production by both small and large phytoplankton at

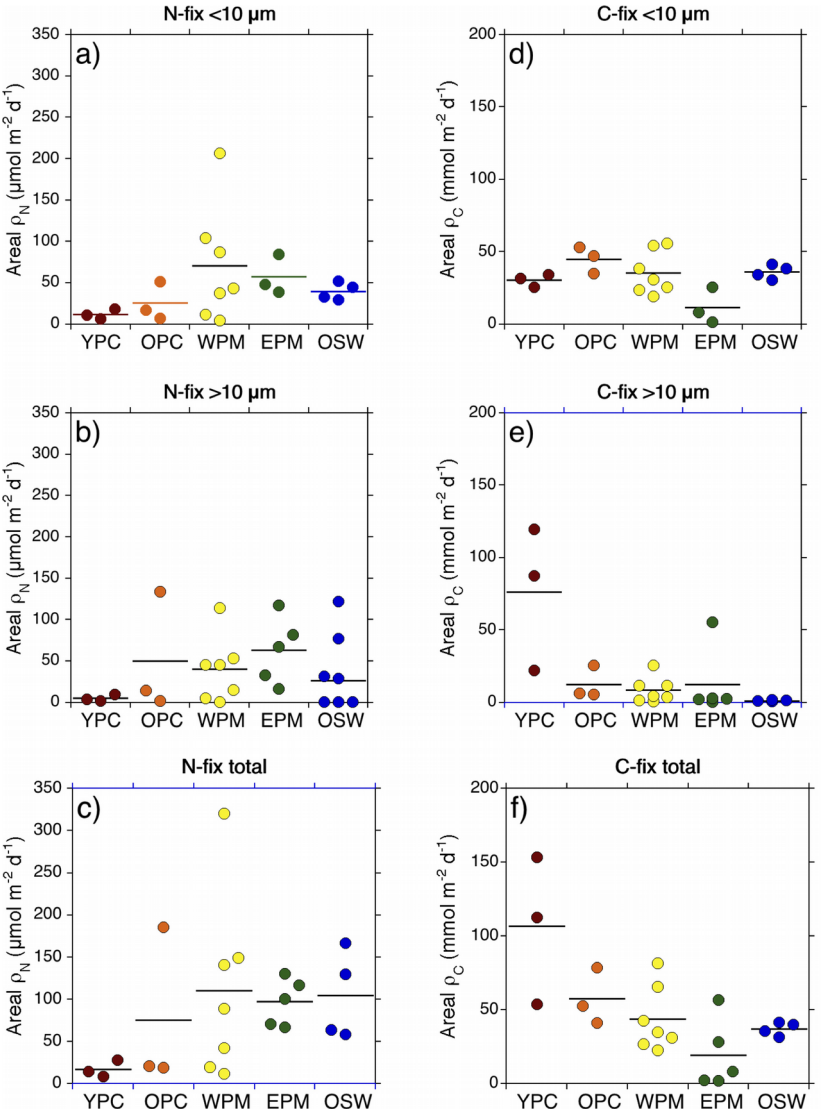

Figure 4. Areal rates of N- and C-fixation by small cells (a, d), large cells (b, e), and the total community (c, f) separated by habitat type. EPM, Eastern Plume Margin; OPC, Old Plume Core; OSW, Offshore Waters; WPM, Western Plume Margin; YPC, Young Plume Core.

EPM stations, where the diazotroph contribution ranged as high as 40% (Fig. 7b, Table 1). Because the large size fraction generally accounted for less biomass than small particles, the diazotroph contribution to total C-fixation was generally modest in all habitat types (Fig. 7b).

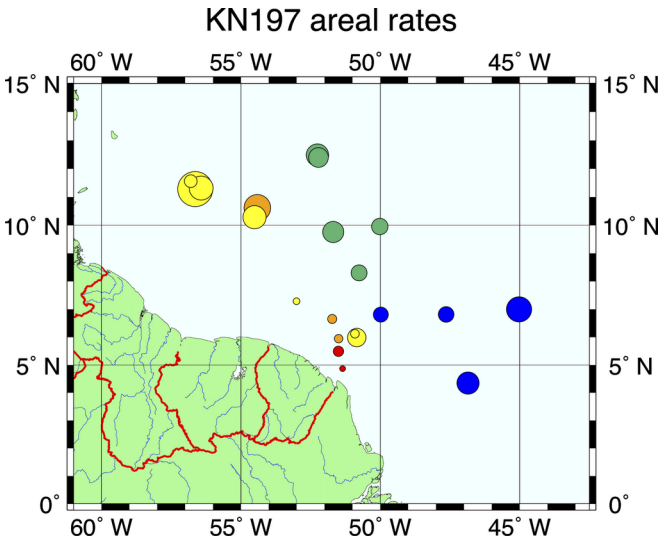

Figure 5. Spatial variation in areal rates of N-fixation. For each station, the symbol area is proportional to the areal rate measured, and symbol color reflects the habitat type as in Weber et al. (2019): red = Young Plume Core (YPC), orange = Old Plume Core (OPC), yellow = Western Plume Margin (WPM), green = Eastern Plume Margin (EPM), and blue = Offshore Waters (OSW).

4. Discussion

Although a number of previous studies have characterized the physical (Muller-Karger, McClain, and Richardson 1988; Longhurst 1993; Muller-Karger, Richardson, and McGillicuddy 1995), biogeochemical (DeMaster and Pope 1996; Subramaniam et al. 2008), and ecological (Smith and Demaster 1996; Foster et al. 2007; Subramaniam et al. 2008) properties of the Amazon River plume, few studies to date have focused on N-fixation rates and the contribution of N-fixation to the planktonic ecosystem. Weber et al. (2017) provide a comprehensive overview of nutrient and particle dynamics during this cruise, Foster et al. (2007, 2011) have discussed diazotroph diversity and distributions in these waters, and Loick-Wilde et al. (2016) have explored the movement of diazotroph nitrogen into the planktonic food web of this system. Here we focus on the spatial distribution of N-fixation in the WTNA and its contribution to the nitrogen budget of these waters in the broader physical and chemical context of the Amazon plume region.

We have presented the overall distribution of hydrographic properties and nutrient concentrations during this cruise in detail elsewhere (Weber et al. 2017) and, more recently, developed a set of criteria for defining pelagic habitats associated with distinct phytoplankton assemblages (Weber et al. 2019). During our cruise, the highly dynamic and variable Amazon plume formed a relatively narrow and coherent band of low-salinity water extending northwest along the coast of South America, and we observed substantial variation in

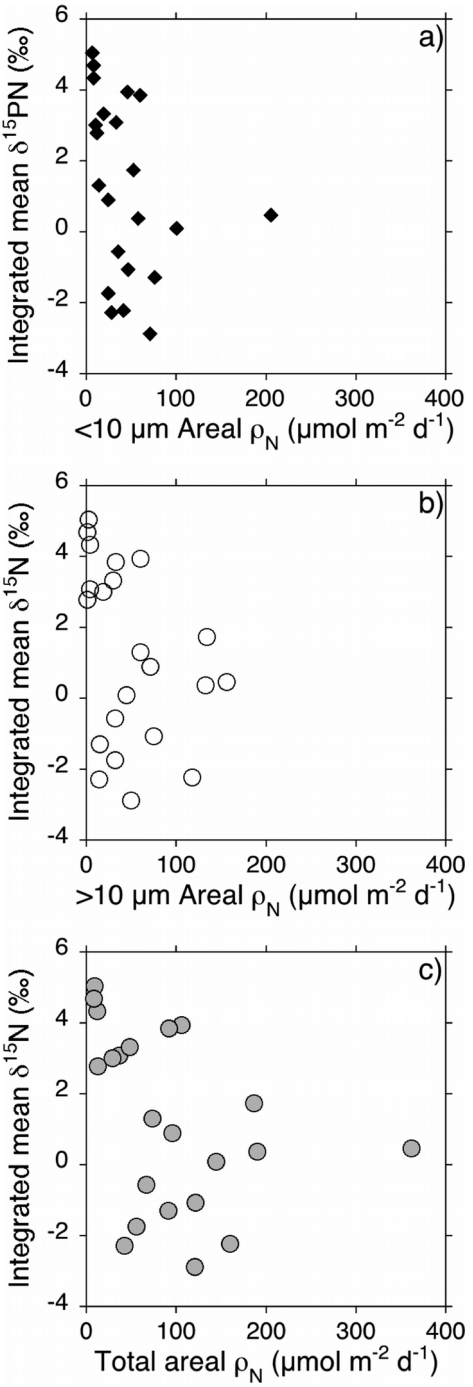

Figure 6. Relationship between mean water column $\delta^{15}N$ of suspended particles and areal rates of N-fixation by the small (< 10 µm) size fraction of particles (a), the large (> 10 µm) size fraction of particles (b), and the total community (c).

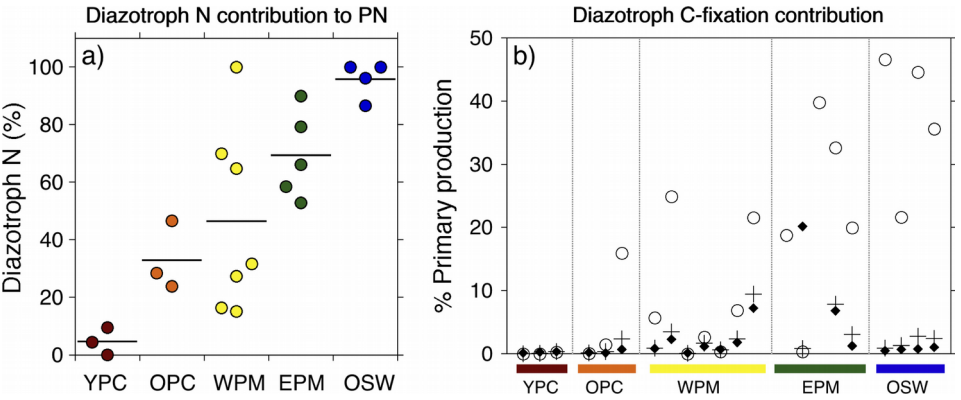

Figure 7. Diazotroph nitrogen contribution to water-column-suspended particles calculated with an isotope mass balance model for each station (circles) with the mean for each habitat type shown with a horizontal bar (a). Percentage of measured rate of C-fixation supported by N-fixation activity assuming Redfield stoichiometry for primary production by small diazotrophs (diamonds), large diazotrophs (circles), and the entire community (crosses). Estimates of the contribution of small diazotrophs to primary production were not available for two EPM stations (b). EPM, Eastern Plume Margin; OPC, Old Plume Core; OSW, Offshore Waters; PN, particulate nitrogen; WPM, Western Plume Margin; YPC, Young Plume Core.

the physical properties of the upper water column on a timescale of hours to days at several of our stations that were occupied for extended periods or were sampled more than once during our cruise. The absence of dissolved inorganic nitrogen in surface waters of most of our stations combined with the presence of significant concentrations of phosphate promoted strong nitrogen limitation of phytoplankton throughout our work area, which in turn created a strong selective pressure favoring diazotrophy (Goes et al. 2014; Weber et al. 2017; Gomes et al. 2018).

a. Distribution of N- and C-fixation

The habitat types we defined for these waters (Weber et al. 2019) are associated with distinct phytoplankton communities (Goes et al. 2014), but our data provide the first opportunity to assess whether critical ecosystem processes are also associated with distinct habitat types. N- and C-fixation rates were detectable, and at times very high, in all habitat types that we sampled on this cruise. These rates varied widely in our work area, and the different habitat types supported patterns of activity that differed qualitatively in terms of vertical distribution and the distribution of N- and C-fixation by the different size classes of phytoplankton (Fig. 2).

In most cases, the volumetric rate of N-fixation was highest at the surface and decreased with depth, reflecting the photoautotrophic nature of N-fixation in this system. The highest rates of N-fixation were associated with the large size fraction of diazotrophs in four of five

habitat types (Fig. 2a–e), which is consistent with previous work documenting the high rates of N-fixation that can be sustained by large diazotrophs such as DDAs and *Trichodesmium* (Capone et al. 1997, 1998, 2005; Carpenter et al. 1999; Sohm et al. 2011). The only habitat type in which the small size fraction of plankton dominated N-fixation was the WPM, which previous studies have shown to be a key site for the development of large populations of active DDAs (Goes et al. 2014; Stukel et al. 2014; Weber et al. 2017).

Rates of C-fixation were highest at/near the surface, with more than an order of magnitude difference in maximal rates among our five habitat types. The Amazon plume clearly plays an important role in providing buoyancy and nutrients to support primary production, resulting in very high rates of C-fixation in the upper 10 m of the water column in the freshest waters we sampled (Fig. 2f). At the other end of our salinity gradient, C-fixation was also highest at the surface, but rates declined rather slowly through the upper 100 m of the water column at OSW stations (Fig. 2j). The highest rates of C-fixation we measured occurred at YPC stations and were about 20-fold higher than the maximum rates we saw at OSW stations. The two habitat types also differed in the nature of the phytoplankton most active in C-fixation, with large cells dominant at YPC stations and small cells at OSW stations. The phytoplankton that were present in other habitat types generally showed C-fixation rates similar to those we observed at OSW stations, and in most cases, the small size fraction accounted for higher rates of C-fixation than the larger phytoplankton, as in the OSW stations.

Areal rates of N- and C-fixation showed clear but distinct trends with salinity. N-fixation by both small and large cells generally increased with salinity for both small and large cells, though we found low rates at all salinities sampled, resulting in a large increase in variance across the salinity gradient we explored (Fig. 3a). In contrast, C-fixation by the small size fraction showed no coherent variation with salinity, whereas C-fixation by large phytoplankton showed a clear decrease with salinity (Fig. 3b). The total rates of N- and C-fixation thus show opposing trends, with both the absolute and the relative contribution of N-fixation increasing from the freshest to the saltiest waters we sampled. This increasing reliance of the planktonic community on N-fixation along the gradient from the plume core to offshore waters is consistent with the apparent release of reactive phosphate as the plume ages that we have previously identified (Weber et al. 2017).

b. Integrative measures of diazotrophy

Our rate measurements provide insight into important biogeochemical processes on a timescale of hours to days, but we have abundant evidence from previous work that documents the dynamic and spatially heterogeneous nature of the Amazon plume system and its phytoplankton communities (Goes et al. 2014; Weber et al. 2017, 2019) and the importance of habitat stability in the development of the distinct communities of diazotrophs and other phytoplankton that drive biogeochemical processes (Stukel et al. 2014). Extrapolating instantaneous rate measurements to longer temporal and spatial scales is always a challenge,

but we can use the $\delta^{15}N$ of suspended particles as an integrative measure of the sources of nitrogen supporting production of biomass on the timescale of particle turnover, which is typically on the order of days to weeks (Montoya 2007; Landrum, Altabet, and Montoya 2011). Specifically, nitrogen stable isotope abundances provide a tool for assessing the relative contribution of diazotrophs to the pool of organic nitrogen in the upper water column.

We previously documented a clear relationship between the abundance of Amazon plume diazotrophs and the $\delta^{15}N$ of suspended particles at the sea surface (Weber et al. 2017), and here we extend this approach to the broader community as represented by the mass- and depth-weighted mean $\delta^{15}PN$ in the upper water column. The mean $\delta^{15}PN$ we found in the upper water column ranged from − 2.9‰ to + 5.0‰, spanning the range of values we used as isotopic end members for this system and suggesting that our choice of isotopic end members was appropriate for characterizing this system. Further, weighted mean $\delta^{15}PN$ values generally scaled inversely with areal rates of N-fixation across all habitat types we sampled (Fig. 6), implying that the instantaneous rates of activity we measured in our 24 h incubations are representative of timescales long enough to affect the bulk pool of suspended particles (days to weeks). In other words, N-fixation is not only widely distributed in the Amazon plume system, but also must have the spatial and temporal persistence to generate a measurable impact on the overall nitrogen budget of the upper water column.

Interestingly, the mean $\delta^{15}N$ of particles showed a stronger dependence on the areal rate of N-fixation by small diazotrophs than on the activity of larger ones (Fig. 6). In both cases, we would expect the mean $\delta^{15}PN$ to asymptotically approach the $\delta^{15}N$ of diazotroph nitrogen (i.e., − 2‰: Montoya, Carpenter, and Capone 2002) as N-fixation increases in importance as a source of new nitrogen supporting primary production. When plotted as a function of areal N-fixation by small diazotrophs (Fig. 6a), the mean $\delta^{15}N$ of suspended particles decreased very strongly from ~ 5‰ to ~ − 2‰ between the lowest rates measured and rates of ~ 100 μmol m^{-2} d^{-1}. In contrast, the mean $\delta^{15}N$ of particles showed a similar decline with large size fraction N-fixation rates up to about 150 μmol m^{-2} d^{-1} (Fig. 6b). This difference suggests that nitrogen fixed by small cells enters the planktonic food web more efficiently than nitrogen fixed by larger cells, perhaps reflecting differences among the grazers feeding on different diazotrophs. This finding is complementary to our previous observations that DDAs have a much stronger impact on the food web and on vertical export than does *Trichodesmium* (Weber et al. 2017) and suggests that the overall coupling between N-fixation and the rest of the planktonic food web is tightest for small particles, intermediate for DDAs, and lowest for *Trichodesmium*.

Our water column mean $\delta^{15}PN$ can be recast into an estimate of the fraction of the standing stock of particulate organic nitrogen that is derived from recent N-fixation ($\%N_{diazo}$) using a simple mixing model (Fig. 7a). Variations in $\%N_{diazo}$ reflect the overall contribution of N-fixation to the base of the food web, and we found $\%N_{diazo}$ values that ranged from near zero at YPC stations to about 100% at OSW stations, with intermediate values at OPC and plume margin (WPM and EPM) stations. This broad range is a clear reflection of the

dynamic and heterogeneous patchwork of planktonic communities and processes that we sampled during this cruise, a source of variation that our habitat type classification can help account for with groupings that reflect biologically relevant aspects of the planktonic ecosystem.

c. Habitat types and rate measurements

We have previously shown that our habitat type approach provides a robust tool for organizing stations in the Amazon plume region into groups that support distinct phytoplankton assemblages and therefore capture key aspects of biologically relevant environmental variation (Weber et al. 2019). Here we extend this approach to physiological rate measurements for the first time to assess whether our habitat types can provide insight into processes and community composition.

We found substantial variability in the spatial distribution of volumetric N- and C-fixation rates among our stations, with clear differences in both the magnitude of our rates and in their vertical distribution (Fig. 2). When grouped by habitat type, we found that the lowest rates of N-fixation occurred at YPC stations in the freshest waters we sampled (Fig. 4a–c), while our highest rates occurred not at the other end of our salinity spectrum, but rather at WPM stations (Fig. 4a–c), though we did observe high rates at EPM and OSW stations as well. Interestingly, some of the highest rates we measured at WPM stations were associated with the small size fraction of particles, which is a clear contrast with our previous work that suggested that the waters these stations sampled are dominated by, and provide a critical habitat for, the development and growth of DDA blooms (Weber et al. 2017). Areal rates of N-fixation by large particles at WPM stations are in fact not very different from those we measured at EPM and OSW stations (Fig. 4b), suggesting that DDAs and *Trichodesmium* were able to fix nitrogen at comparable rates everywhere except for the core of the plume proper. We have not yet identified the small organisms responsible for the high rates of N-fixation at our WPM stations, and it is of course possible that this partitioning of activity is an artifact arising through cell breakage and fragmentation during the filtrations that terminated our incubations, but there is no obvious reason that these stations should be affected by this problem more strongly than other nearby stations (e.g., Fig. 1b), suggesting that our finding is not likely to be a simple handling artifact.

C-fixation rates showed a somewhat simpler pattern of variation in our system (Fig. 4d–f), with little variation among habitat types in C-fixation by the small size fraction and very high rates of C-fixation by the large size fraction in the freshest waters sampled (YPC stations). In general, overall rates of C-fixation decreased from the core to the margins of the plume and offshore waters (Fig. 4d–f). The dominance of the large size fraction of primary producers at YPC stations is consistent with the abundant populations of coastal diatoms we found there (Goes et al. 2014), many of which are chain formers.

We found a number of interesting contrasts in the relative contributions of the two size fractions of particles to N- and C-fixation. For example, N-fixation at our OSW stations

tended to be higher in the large than in the small size fraction of particles (Fig. 2e), while the small cells clearly accounted for much higher rates of C-fixation than the large cells (Fig. 2j). Mismatches in activity like this imply that nitrogen and carbon enter and presumably move through the planktonic system through different pathways, providing opportunities for partial decoupling of these two elemental cycles.

Integration of our rates through the upper water column provides a useful measure of the potential ecosystem impact of diazotrophy in different habitat types. N-fixation by the small size fraction of plankton showed a clear contrast between the very low rates we measured in the plume core (YPC and OPC; Fig. 4a) and the generally higher rates in the other habitats. The large size fraction of plankton showed very uniform ranges of areal N-fixation in the plume margin and offshore water stations (WPM, EPM, and OSW; Fig. 4b). The total rate of N-fixation showed an even clearer contrast between the plume and other waters. In fact, only one plume-associated station (OPC Station 023; Fig. 1a) showed high rates of N-fixation. This station was in a very dynamic and heterogeneous region, and we may have sampled the station as it transitioned toward the WPM habitat type (Weber et al. 2019).

Taken together, our areal rate measurements show a relatively simple pattern of increasing N-fixation activity along a habitat type sequence from the plume core to the plume margins and offshore waters (Figs. 4 and 5). Among our habitat types, WPM stands out as unusual in several respects: it is the only habitat type in which the small size fraction of particles supported the highest rates of both N- and C-fixation (Fig. 2), and it shows the greatest range of areal N-fixation by small particles and by the entire diazotroph community among our five habitat types. The importance of the small size fraction of diazotrophs was unexpected given the previous focus we and others have had on this region as a hot spot for the development and growth of DDA blooms (Goes et al. 2014; Weber et al. 2017).

d. Habitat types and diazotroph impact

We used two distinct approaches to assess the diazotroph contribution to the phytoplankton community on experimental and longer timescales. First, we used the mean $\delta^{15}N$ of suspended particles in the upper water column as a measure of the overall contribution of diazotrophy to the planktonic nitrogen budget on ecological timescales. This isotopic metric integrates the particulate organic nitrogen accumulated over time and space as the suspended particles were moved by the local circulation. Our data show strong contrasts among the five habitat types and a coherent pattern of increasing $\%N_{diazo}$ along our habitat type sequence from the plume core to the plume margins and offshore waters (Fig. 7a). We found clear separations among the means and relatively little variance within each habitat type with the obvious exception of the WPM habitat type, which included stations spanning a range from the plume core habitats to the highest values we measured in offshore waters. The seven stations in this habitat type appear to fall into two clusters, one centered around $\%N_{diazo}$ values of about 25% and comparable to our plume core stations, and the other loosely centered around N_{diazo} values of about 80% and similar to our EPM stations.

As noted previously, our WPM stations show unusual variation in the magnitude and partitioning of volumetric rates of N- and C-fixation between size fractions. Taken together, our data support earlier suggestions that the waters to the west of the plume core (i.e., our WPM habitat type) exemplify a dynamic and highly variable frontal region in which planktonic communities are responding to changes in their physical and chemical environment driven by advective and turbulent processes, producing an unusual degree of biological heterogeneity in this region.

We complemented this isotopic assessment of the role of diazotrophs in supplying nitrogen to suspended particles by calculating the percentage of primary production (C-fixation rate) that could be supported by N-fixation using Redfield stoichiometry. This approach provides a direct estimate of the contribution of diazotrophs to primary production on the timescale of our experiments (1 d). At most of our stations, N-fixation could support only a few percent of the total nitrogen demand of C-fixation by small phytoplankton or the total phytoplankton community, though several plume margin stations had N-fixation rates high enough to supply a substantial fraction of the primary production nitrogen demand (Fig. 7b, Table 1). Interestingly, large diazotrophs often made a substantial contribution to the nitrogen demand of primary production by large cells, in keeping with the high population densities that both DDAs and *Trichodesmium* can attain in this system (e.g., Goes et al. 2014; Gomes et al. 2018).

Our two estimates of diazotroph contribution to the plankton focus on very different aspects of the ecosystem: stable isotope abundances that integrate the inputs of nitrogen to the system through time (Fig. 7a) and rates measured in 24 h long experiments (Fig. 7b). Even the highest estimated contributions of diazotrophy to total primary production (EPM stations; Fig. 7b) were much lower than the corresponding estimates of diazotroph contributions to water column particulate organic matter (EPM Stations; Fig. 7a). Our instantaneous rate comparisons imply that remineralized production dominates in all our habitat types, while diazotrophic new production is most important in plume margin habitats. In contrast, our isotope budget implies that diazotroph nitrogen can account for most or all of the standing stock of suspended particulate organic nitrogen at plume margin (WPM and EPM) and OSW stations, with substantial contributions of diazotroph nitrogen even at OPC stations. This clear difference between our instantaneous and integrative estimates of diazotroph contributions implies that carbon and nitrogen are following distinct paths through the system, with much greater remineralization of carbon than of nitrogen. This allows even modest inputs of diazotroph nitrogen relative to total primary production to accumulate in the plankton over time and highlights the critical role of diazotrophy as an ecosystem service in the WTNA and other marine planktonic systems.

5. Conclusions

We have used a combination of focused experimental rate measurements (N- and C-fixation) and integrative isotopic measurements of the contribution of N-fixation to the

pool of suspended particles to assess phytoplankton community activity in the portion of the WTNA affected by the Amazon plume. This combination of nitrogen stable isotope tracer and natural abundance approaches brought together tools and approaches used by biological oceanographers and biogeochemists and was pioneered by James McCarthy and his lab group in the 1980s and 1990s in studies of diverse estuarine and offshore waters (e.g., Altabet and McCarthy 1986; McCarthy and Nevins 1986a, 1986b; Horrigan et al. 1990a,1990b; Montoya, Horrigan, and McCarthy 1990, 1991; McCarthy, Garside, and Nevins 1992; Montoya, Wiebe, and McCarthy 1992). Simultaneous use of tracer and natural abundance isotope measurements requires great care to avoid cross contamination but provides the opportunity to study ecosystem processes on a broad range of biologically and ecologically relevant timescales.

One interesting outcome of our use of tracer and natural abundance approaches was a striking contrast between our experimentally based estimates of the fraction of primary production that could be supported by N-fixation and our stable isotope budgets. Our rate measurements show that remineralized production dominated the system and that N-fixation typically supported only a few percent of total primary production. In contrast, our isotope budget clearly showed that diazotrophy was the dominant source of the PN in the water column, highlighting both the integrative nature of this measurement and the very different fates of carbon and nitrogen in the plankton, with nitrogen being retained in the system much more efficiently than carbon.

We complemented these rate and isotopic measurements with a recently described approach for delineating phytoplankton habitats using a simple set of parameters that are routinely measured during oceanographic cruises. Our findings provide strong evidence that these simply defined habitat types can not only help in defining phytoplankton communities but also provide insight into the distribution and impact of important biogeochemical processes carried out by those phytoplankton communities (e.g., N-fixation).

Both aspects of our habitat type analysis are important—one of our primary findings here is that N-fixation by the small size fraction of particles appears to contribute to the PN pool of the upper water column more directly than N-fixation by larger phytoplankton. This conclusion is complementary to our previous finding that DDAs and *Trichodesmium* contribute to the food web and vertical export in very different ways (Weber et al. 2017) and highlights the importance of community composition and structure in determining the impacts of a common biogeochemical pathway.

Acknowledgments. We thank the officers and crew of the R/V *Knorr* for their assistance and support in our work at sea. We also thank Erica Strope, Rachel Horak, Julia Grosse, and Julie Gonzalez for their assistance at sea and in the laboratory. Most importantly, we extend our sincerest thanks to Jim McCarthy for his years of leadership and his care in mentoring young scientists. This research was supported by grants NSF-OCE-0934025 and NSF-OCE-1737078 to JPM.

REFERENCES

Altabet, M. A., and J. J. McCarthy. 1986. Vertical patterns in ^{15}N natural abundance in PON from the surface waters of warm-core rings. J. Mar. Res., *44*, 185–201. doi: 10.1357/002224086788460148

Berthelot, H., T. Moutin, S. L'Helguen, K. Leblanc, S. Helias, O. Grosso, N. Leblond, B. Charrière, and S. Bonnet. 2015. Dinitrogen fixation and dissolved organic nitrogen fueled primary production and particulate export during the VAHINE mesocosm experiment (New Caledonia lagoon). Biogeosciences, *12*(13), 4099–4112. doi: 10.5194/bg-12-4099-2015

Calef, G. W., and G. D. Grice. 1967. Influence of the Amazon River outflow on the ecology of the western tropical Atlantic. II. Zooplankton abundance, copepod distribution, with remarks on the fauna of low-salinity areas. J. Mar. Res., *25*(1), 84–94.

Capone, D. G., J. A. Burns, J. P. Montoya, A. Subramaniam, C. Mahaffey, T. Gunderson, A. F. Michaels, and E. J. Carpenter. 2005. Nitrogen fixation by *Trichodesmium* spp.: An important source of new nitrogen to the tropical and subtropical North Atlantic Ocean. Global Biogeochem. Cycles, *19*, GB2024. doi: 10.1029/2004GB002331

Capone, D. G., A. Subramaniam, J. P. Montoya, M. Voss, C. Humborg, A. M. Johansen, R. L. Siefert, and E. J. Carpenter. 1998. An extensive bloom of the N_2-fixing cyanobacterium *Trichodesmium erythraeum* in the central Arabian Sea. Mar. Ecol. Prog. Ser., *172*, 281–292. doi: 10.3354/meps172281

Capone, D. G., J. P. Zehr, H. W. Paerl, B. Bergman, and E. J. Carpenter. 1997. *Trichodesmium*, a globally significant marine cyanobacterium. Science, *276*(5316), 1221–1229. doi: 10.1126/science.276.5316.1221

Carpenter, E. J., J. P. Montoya, J. Burns, M. R. Mulholland, A. Subramaniam, and D. G. Capone. 1999. Extensive bloom of a N_2-fixing diatom/cyanobacterial association in the tropical Atlantic Ocean. Mar. Ecol. Prog. Ser., *185*, 273–283. doi: 10.3354/meps185273

Carpenter, E. J., A. Subramaniam, and D. G. Capone. 2004. Biomass and productivity of the cyanobacterium *Trichodesmium* spp. in the tropical N Atlantic Ocean. Deep-Sea Res., Part I, *51*, 173–203. doi: 10.1016/j.dsr.2003.10.006

Coles, V. J., M. T. Brooks, J. Hopkins, M. R. Stukel, P. L. Yager, and R. R. Hood. 2013. The pathways and properties of the Amazon River Plume in the tropical North Atlantic Ocean. J. Geophys. Res.: Oceans, *118*(12), 6894–6913. doi: 10.1002/2013jc008981

Conroy, B. J., D. K. Steinberg, M. R. Stukel, J. I. Goes, and V. J. Coles. 2016. Meso- and microzooplankton grazing in the Amazon River plume and western tropical North Atlantic. Limnol. Oceanogr., *61*(3), 825–840. doi: 10.1002/lno.10261

Del Vecchio, R., and A. Subramaniam. 2004. Influence of the Amazon River on the surface optical properties of the western tropical North Atlantic Ocean. J. Geophys. Res., *109*, C11001. doi: 10.1029/2004JC002503

DeMaster, D., and R. H. Pope. 1996. Nutrient dynamics in Amazon shelf waters: Results from AMASSEDS. Cont. Shelf Res., *16*, 263–289. doi: 10.1016/0278-4343(95)00008-O

Foster, R. A., M. M. M. Kuypers, T. Vagner, R. W. Paerl, N. Musat, and J. P. Zehr. 2011. Nitrogen fixation and transfer in open ocean diatom-cyanobacterial symbioses. ISME J., *5*(9), 1484–1493. doi: 10.1038/ismej.2011.26

Foster, R. A., A. Subramaniam, C. Mahaffey, E. J. Carpenter, D. G. Capone, and J. P. Zehr. 2007. Influence of the Amazon River plume on distributions of free-living and symbiotic cyanobacteria in the western tropical north Atlantic Ocean. Limnol. Oceanogr., *52*, 517–532. doi: 10.4319/lo.2007.52.2.0517

Glibert, P. M., and D. A. Bronk. 1994. Release of dissolved organic nitrogen by marine diazotrophic cyanobacteria, *Trichodesmium* spp. Appl. Environ. Microbiol., *60*(11), 3996–4000.

Goes, J. I., H. D. R. Gomes, A. M. Chekalyuk, E. J. Carpenter, J. P. Montoya, V. J. Coles, P. L. Yager, et al. 2014. Influence of the Amazon River discharge on the biogeography of phytoplankton communities in the western tropical North Atlantic. Prog. Oceanogr., *120*, 29–40. doi: 10.1016/J.Pocean.2013.07.010

Gomes, H. D., Q. Xu, J. Ishizaka, E. J. Carpenter, P. L. Yager, and J. I. Goes. 2018. The influence of riverine nutrients in niche partitioning of phytoplankton communities – a contrast between the Amazon River Plume and the Changjiang (Yangtze) River diluted water of the East China Sea. Front. Mar. Sci., *5*, 343. doi: 10.3389/fmars.2018.00343

Grosskopf, T., W. Mohr, T. Baustian, H. Schunck, D. Gill, M. M. Kuypers, G. Lavik, R. A. Schmitz, D. W. R. Wallace, and J. LaRoche. 2012. Doubling of marine dinitrogen-fixation rates based on direct measurements. Nature, *488*(7411), 361–364. doi: 10.1038/nature11338

Horrigan, S. G., J. P. Montoya, J. L. Nevins, and J. J. McCarthy. 1990a. Natural isotopic composition of dissolved inorganic nitrogen in the Chesapeake Bay. Estuarine, Coastal Shelf Sci., *30*, 393–410. doi: 10.1016/0272-7714(90)90005-C

Horrigan, S. G., J. P. Montoya, J. L. Nevins, J. J. McCarthy, H. W. Ducklow, R. Goericke, and T. Malone. 1990b. Nitrogenous nutrient transformations in the spring and fall in the Chesapeake Bay. Estuarine, Coastal Shelf Sci., *30*, 369–391. doi: https://doi.org/10.1016/0272-7714(90)90004-B

Hu, C. M., E. T. Montgomery, R. W. Schmitt, and F. E. Muller-Karger. 2004. The dispersal of the Amazon and Orinoco River water in the tropical Atlantic and Caribbean Sea: Observation from space and S-PALACE floats. Deep-Sea Res., Part II, *51*(10–11), 1151–1171. doi: 10.1016/j.dsr2.2004.04.001

Johns, W. E., T. N. Lee, F. A. Schott, R. J. Zantopp, and R. H. Evans. 1990. The North Brazil Current retroflection: Seasonal structure and eddy variability. J. Geophys. Res.: Oceans, *95*(C12), 22103–22120. doi: 10.1029/JC095iC12p22103

Landrum, J. P., M. A. Altabet, and J. P. Montoya. 2011. Basin-scale distributions of stable nitrogen isotopes in the subtropical North Atlantic Ocean: Contribution of diazotroph nitrogen to particulate organic matter and mesozooplankton. Deep-Sea Res., Part I, *58*(5), 615–625. doi: 10.1016/j.dsr.2011.01.012

Loick-Wilde, N., S. C. Weber, B. J. Conroy, D. G. Capone, V. J. Coles, P. M. Medeiros, D. K. Steinberg, and J. P. Montoya. 2016. Nitrogen sources and net growth efficiency of zooplankton in three Amazon River plume food webs. Limnol. Oceanogr., *61*(2), 460–481. doi: 10.1002/lno.10227

Longhurst, A. 1993. Seasonal cooling and blooming in tropical oceans. Deep-Sea Res., Part I, *40*, 2145–2165. doi: 10.1016/0967-0637(93)90095-K

McCarthy, J. J., C. Garside, and J. L. Nevins. 1992. Nitrate supply and phytoplankton uptake kinetics in the euphotic layer of a Gulf Stream warm-core ring. Deep-Sea Res., Part A, *39*(S1), S393–S403. doi: 10.1016/S0198-0149(11)80021-X

McCarthy, J. J., and J. L. Nevins. 1986a. Sources of nitrogen for primary production in warm-core rings 79-E and 81-D. Limnol. Oceanogr., *31*, 690–700. doi: 10.4319/lo.1986.31.4.0690

McCarthy, J. J., and J. L. Nevins. 1986b. Utilization of nitrogen and phosphorus by primary producers in warm-core ring 82-B following deep convective mixing. Deep-Sea Res., Part A, *33*, 1773–1788. doi: 10.1016/0198-0149(86)90079-8

Mohr, W., T. Grosskopf, D. W. R. Wallace, and J. LaRoche. 2010. Methodological underestimation of oceanic nitrogen fixation rates. PLoS ONE, *5*(9), e12583. doi: 10.1371/journal.pone.0012583

Molleri, G. S. F., E. M. L. D. Novo, and M. Kampel. 2010. Space-time variability of the Amazon River plume based on satellite ocean color. Cont. Shelf Res., *30*(3–4), 342–352. doi: 10.1016/j.csr.2009.11.015

Montoya, J. P. 2007. Natural abundance of ^{15}N in marine planktonic ecosystems, *in* Stable Isotopes in Ecology and Environmental Science, 2nd ed., R. Michener and K. Lajtha, eds. Malden, MA: Blackwell, 176–201.

Montoya, J. P. 2008. Nitrogen stable isotopes in marine environments, *in* Nitrogen in the Marine Environment, D. G. Capone, E. J. Carpenter, M. R. Mulholland, and D. A. Bronk, eds. Burlington, MA: Academic Press, 1277–1302.

Montoya, J. P., E. J. Carpenter, and D. G. Capone. 2002. Nitrogen-fixation and nitrogen isotope abundances in zooplankton of the oligotrophic North Atlantic. Limnol. Oceanogr., *47*, 1617–1628. doi: 10.4319/lo.2002.47.6.1617

Montoya, J. P., S. G. Horrigan, and J. J. McCarthy. 1990. Natural abundance of ^{15}N in particulate nitrogen and zooplankton in the Chesapeake Bay. Mar. Ecol. Prog. Ser., *65*(1), 35–61. doi: 10.3354/meps065035

Montoya, J. P., S. G. Horrigan, and J. J. McCarthy. 1991. Rapid, storm-induced changes in the natural abundance of ^{15}N in a planktonic ecosystem, Chesapeake Bay, USA. Geochim. Cosmochim. Acta, *55*, 3627–3638. doi: 10.1016/0016-7037(91)90060-i

Montoya, J. P., M. Voss, P. Kahler, and D. G. Capone. 1996. A simple, high-precision, high-sensitivity tracer assay for N_2 fixation. Appl. Environ. Microbiol., *62*(3), 986–993.

Montoya, J. P., P. H. Wiebe, and J. J. McCarthy. 1992. Natural abundance of ^{15}N in particulate nitrogen and zooplankton in the Gulf Stream region and warm-core ring 86A. Deep-Sea Res., Part A, *39*(S1), S363–S392. doi: 10.1016/S0198-0149(11)80020-8

Muller-Karger, F. E., C. R. McClain, and P. L. Richardson. 1988. The dispersal of the Amazon's water. Nature, *333*, 56–59.

Muller-Karger, F. E., P. L. Richardson, and D. McGillicuddy. 1995. On the offshore dispersal of the Amazon's Plume in the North Atlantic. Deep-Sea Res., Part I, *42*(11–12), 2127–2131, 2133–2137. doi: 10.1016/0967-0637(95)00085-2

Parsons, T. R., Y. Maita, and C. M. Lalli. 1984. A Manual of Chemical and Biological Methods for Seawater Analysis. Oxford, UK: Pergamon Press.

Ryther, J. H., D. W. Menzel, and N. Corwin. 1967. Influence of the Amazon River outflow on the ecology of the western tropical Atlantic. I. Hydrography and nutrient chemistry. J. Mar. Res., *25*(1), 69–83.

Sigman, D. M., M. A. Altabet, D. C. McCorkle, R. François, and G. Fischer. 2000. The $\delta^{15}N$ of nitrate in the Southern Ocean: Nitrogen cycling and circulation in the ocean interior. J. Geophys. Res., *105*, 19599–19614. doi: 10.1029/2000JC000265

Smith, W. O., and D. J. Demaster. 1996. Phytoplankton biomass and productivity in the Amazon River plume: Correlation with seasonal river discharge. Cont. Shelf Res., *16*(3), 291–319. doi: 10.1016/0278-4343(95)00007-N

Sohm, J. A., A. Subramaniam, T. E. Gunderson, E. J. Carpenter, and D. G. Capone. 2011. Nitrogen fixation by *Trichodesmium* spp. and unicellular diazotrophs in the North Pacific Subtropical Gyre. J. Geophys. Res.: Biogeosci., *116*, G03002. doi: 10.1029/2010JG001513

Stukel, M. R., V. J. Coles, M. T. Brooks, and R. R. Hood. 2014. Top-down, bottom-up and physical controls on diatom-diazotroph assemblage growth in the Amazon River plume. Biogeosciences, *11*(12), 3259–3278. doi: 10.5194/bg-11-3259-2014

Subramaniam, A., P. L. Yager, E. J. Carpenter, C. Mahaffey, K. Bjorkman, S. Cooley, A. B. Kustka, et al. 2008. Amazon River enhances diazotrophy and carbon sequestration in the tropical North Atlantic Ocean. Proc. Natl. Acad. Sci. U. S. A., *105*(30), 10460–10465. doi: 10.1073/pnas.0710279105

Vorosmarty, C., B. Fekete, M. Meybeck, and R. Lammers. 2000. Global system of rivers: Its role in organizing continental land mass and defining land-to-ocean linkages. Global Biogeochem. Cycles, *14*, 599–621. doi: 10.1029/1999GB900092

Wannicke, N., M. Benavides, T. Dalsgaard, J. W. Dippner, J. P. Montoya, and M. Voss. 2018. New perspectives on nitrogen fixation measurements using $^{15}N_2$ gas. Front. Mar. Sci., *5*, 120. doi: 10.3389/fmars.2018.00120

Weber, S. C., E. J. Carpenter, V. J. Coles, P. L. Yager, J. Goes, and J. P. Montoya. 2017. Amazon River influence on nitrogen fixation and export production in the western tropical North Atlantic. Limnol. Oceanogr., *62*(2), 618–631. doi: 10.1002/lno.10448

Weber, S. C., A. Subramaniam, J. P. Montoya, D. N. Hai, N. N. Lam, J. W. Dippner, and M. Voss. 2019. Habitat delineation in highly variable marine environments. Front. Mar. Sci. *6*, 112. doi: 10.3389/fmars.2019.00112

Yeung, L. Y., W. M. Berelson, E. D. Young, M. G. Prokopenko, N. Rollins, V. J. Coles, J. P. Montoya, et al. 2012. Impact of diatom-diazotroph associations on carbon export in the Amazon River plume. Geophys. Res. Lett., *39*, L18609. doi: 10.1029/2012gl053356

Received: *1 May 2019*; revised: *28 June 2019*.